
Article:

Wang, Z, Maotsela, T, Toperesu, PM et al. (3 more authors) (2019) Dynamic and static corrosion of alpha-alumina bonded refractory in contact with molten soda-lime-silica (SLS) glass. Ceramics International, 45 (1). pp. 725-732. ISSN 0272-8842

https://doi.org/10.1016/j.ceramint.2018.09.235

Dynamic and static corrosion of alpha-alumina bonded refractory in contact with molten soda-lime-silica (SLS) glass

Zihua Wang,[a,b] Tlamelo Maotsela,[a] Phillip M Toperesu[a]; Girish M. Kale,[a,]* Jafar Daji[b] and David Parkinson[b]

[a]Institute for Materials Research, School of Process, Environmental and Materials Engineering, University of Leeds, Leeds LS2 9JT, U.K.

[b]Parkinson-Spencer Refractories Ltd, Halifax HX3 6SX, U.K.

*Author for all correspondences: g.m.kale@leeds.ac.uk (E); 0044-113-3432805 (T)

Abstract

The corrosion behaviour of sintered high purity α-Al2O3 refractory composition in contact with soda-lime-silicate (SLS) glass has been investigated using a dynamic corrosion test designed to simulate industrial conditions. Experiments were conducted as function of rotation speed, contact time duration and temperature. The results of dynamic corrosion tests are in excellent agreement with those obtained from static crucible test at 1370 °C for 72 hours which is a standard industrial testing practice. The phase composition and microstructures of the glass-refractory interface of these samples were studied by X-ray Diffraction (XRD) and combined Scanning Electron Microscopy – Energy Dispersive X-ray Spectroscopy (SEM-EDS), respectively. Elemental mapping was also carried out on the glass-refractory interface.

Keywords: B. characterisation **C.** static/dynamic corrosion, **D.** soda-lime silica glass, **E.** High-temperature; **E.** refractories,

1 Introduction

Refractories are structural materials which are required to retain high strength and be physically and chemically stable at operating temperatures, for this reason they are used in the glass, cement and metals industry for various purposes at high temperature in aggressive environments. In the container-glass manufacturing process, refractories of different compositions are widely used in the furnace, distributor, forehearth channels, and in parts such as plungers, spouts, tubes, stirrers, rotor segments, mantle blocks and orifice rings [1].

The physical and chemical properties of refractories that are in direct contact with molten glass plays a key role in the determination of the quality of glass products. During their lifetime, the refractories are exposed to chemically aggressive nature of the molten glass and, even more importantly to thermal and mechanical stresses. Hence, the refractory materials that are in contact with glass at elevated temperatures must have excellent chemical and mechanical stability [2]. Alumina is one of the most important refractory materials in glass furnaces due to its high melting point, good mechanical properties such as high hardness, high compressive strength, high elastic modulus and, good chemical and thermal stability [3-8].

Dense sintered alumina has been used for many years for pyrometer sheaths and other high temperature applications. However, large sections of bonded alumina refractories were not being used in glass industry until the 1960s'. It has been found that the high alumina refractories are durable in glass production and melting furnaces and, in contact with special lead containing alkali metal silicate glasses, because of its high corrosion resistance [5-8]. The temperature of the molten glass in production channel designed for feeding molten glass for forming is between 1000 and 1350 ºC [1, 2] depending on the composition of glass. Molten glass attacks refractory in a complex manner involving not only chemical corrosion, but also physical wear, such as erosion or abrasion.

The chemical corrosion and physical wear may act synergistically in determining the overall refractory corrosion and wear [6, 7]. The corrosion resistance of any refractory material, characterized by the rate of dissolution of the refractory into a molten glass, is dependent on several factors [6-8]. These include the refractory chemical composition, phase relations, relative thermodynamic stabilities of oxide components of glass and refractories, micro-structural features of the refractory, temperature, composition of molten glass, viscosity of the molten glass and flow rate of the molten glass. To determine the corrosion resistance of various refractories, two different methods such as dynamic [6, 7] and static [9] have been widely employed. Static crucible test of bonded Al_2O_3-ZrO_2-SiO_2 (AZS) refractory using standard soda-lime-silica (SLS) glass at 1370 ºC for 72 hrs have been performed by Aksel [9]. The corrosion behaviour and microstructures of fused cast AZS and Cr_2O_3-based refractories were analysed by Pena et al. [6, 7] using dynamic corrosion test at about 1500 ºC for 24 hrs. Although there have been several studies on alumina based refractory materials, only a few reports exist in the literature on the corrosion behaviour of alumina refractories employed in glass making processes.

In this investigation, the corrosion rate of a high purity bonded alumina refractory has been studied using both dynamic corrosion testing and static crucible testing at elevated temperatures. The glass-refractory contact surfaces of the test samples before and after dynamic corrosion test have been analysed using X-ray diffraction (XRD) for their phase constitution. Furthermore, the microstructures of the test samples have been observed using Scanning Electron Microscopy (SEM) and analysed employing Energy Dispersive X-ray Spectroscopy (EDS). A detailed account of the research work and its findings are described in the following sections.

2 Experimental

2.1 Materials

Commercial high purity α-Al_2O_3 refractory samples named as PSR-993 (Parkinson-Spencer Refractories Ltd, Halifax, UK) were used in this study. The alumina refractory sample is a sintered block fabricated by the slip casting technique. Commercial soda-lime-silica (SLS) cullet commonly used in the manufacture of glass bottles and containers were purchased from Berryman Ltd (South Kirkby, UK). The main chemical constituents of both glass and refractory samples determined by X-ray Fluorescence spectroscopy (XRF) are given in Table 1.

Table 1. Chemical constituents of the soda-lime silica glass and PSR-993 test specimen.

Oxides wt%	**SiO_2**	**Na_2O**	**CaO**	**Al_2O_3**	**MgO**	**K_2O**	**Others**
SLS	71.53	12.78	10.78	1.53	1.41	0.59	1.38
PSR-993	-	-	-	99.70	-	-	0.30

2.1 Dynamic Corrosion Test

A specially designed and fabricated apparatus for the dynamic corrosion test has been used in this investigation [10, 11]. A top loading furnace (Lenton Thermal Designs Ltd, Market Harborough, UK) was employed for melting glass during the dynamic corrosion test at different temperatures. Before the experiment, an Al_2O_3-ZrO_2-SiO_2 (AZS) crucible filled with 600g cullet was placed inside the furnace and heated to the desired temperature. An adjustable frame connected by a winch was used to control the lowering or lifting of the sample position before and after the experiment, respectively. The rotation speed was controlled by a motor (Parvalux Electric Motor Ltd, Dorset, UK), which was mounted on the adjustable sample holder frame. In order to avoid over-heating of the motor, a stainless-steel shaft was used to connect the motor and, the ceramic sample holder and ceramic shaft. A supporting bar with a ball bearing was used to maintain a stable position of the rotating shaft and sample holder assembly during the experiment. An alumina plate, with four holes to place the test samples, was used as a sample holder, as shown in Figure 1A and 1B, respectively. The samples for the experiments were core drilled from PSR-993 refractory block to a specific shape and size. Each of the samples was cylindrical in shape with 100 (±0.02) mm lengths and 15 (±0.02) mm diameters. For each corrosion test run, four finger samples were fixed into position to the corresponding holes in the sample holder using refractory clay. Fibre insulation was placed around the keyhole opening to prevent heat loss so as to maintain constant temperature during experiment (see Figure 1A).

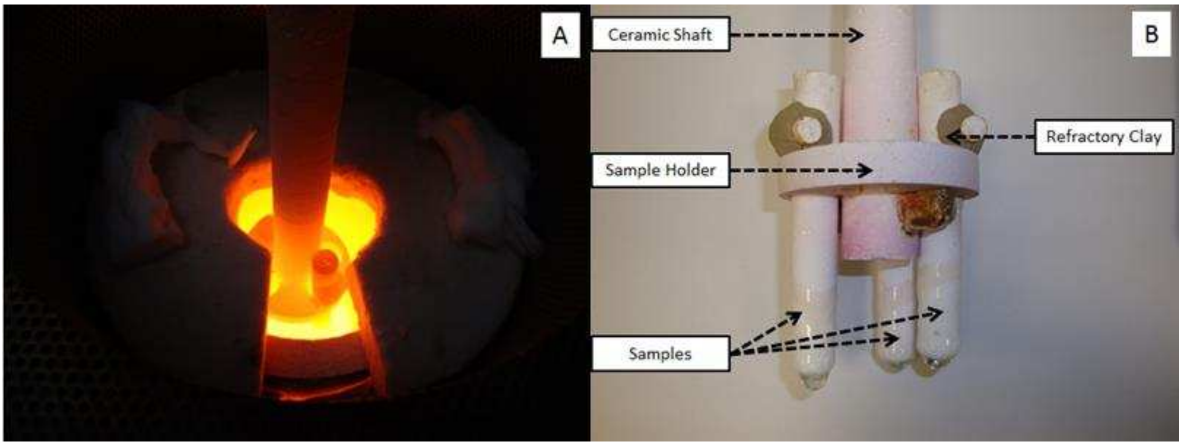

Figure 1: Part of the dynamic corrosion test rig. **A** is PSR-993 samples about to be immersed in molten SLS glass at 1370 ºC during dynamic corrosion test and **B** is the ceramic sample holder with PSR-993 fingers being withdrawn from molten glass after dynamic corrosion test, respectively.

The corrosion tests were conducted as a function of temperature and rotation speed. Once the desired test temperature was attained the PSR-993 refractory finger samples mounted on the sample holder (Figure 1B) were lowered into the molten glass using the adjustable frame. The test temperatures used were 1370 ºC, 1420 ºC, 1460 ºC and 1470 ºC, with heating and cooling rate of 180 ºC/hr, respectively. The rotation speeds used were 0, 5, 10, 12 and 15 rpm, which corresponds to a linear flow rate of 0, 628, 1256, 1507 and 1884 mm min-1 of molten glass, respectively. Note that the standard glass flow is typically 180 mm min-1 in glass industry. The testing time length was also fixed at 24, 48, 53 and 72 hrs, respectively. Once the corrosion test was complete for a given set of parameters, the sample holder was raised and the glass melt coating the finger samples allowed to drip under gravity for an hour before cooling down to room temperature for further characterization.

In this study, the “Before and After” material loss method was used to evaluate the corrosion rate of the finger samples under dynamic conditions. The diameters of the melt line regions of the test samples before and after the corrosion tests were measured and the materials loss calculated. 4 specimen samples tested at 1370 ºC for 72 hours without rotation (0 rpm) were used as a reference with corrosion index = 1.

The reference state is based on the ASTM standard in the literature [12]. The corrosion index for test piece A was identified as:

$$Corrosion\ index\ for\ test\ sample\ A = \frac{\left[\pi\left(\frac{D_i}{2}\right)^2 \Delta l - \pi\left(\frac{D_f}{2}\right)^2 \Delta l\right]_A}{\left[\pi\left(\frac{D_i}{2}\right)^2 \Delta l - \pi\left(\frac{D_f}{2}\right)^2 \Delta l\right]_F} = \frac{(D_i - D_f)_A^2}{(D_i - D_f)_F^2} \quad (1)$$

Where, $\mathbf{D}_i$ and $\mathbf{D}_f$; are the initial and final diameters of each specimen sample, respectively. Δl is the length of the specimen. **A** and **F** stands for the test sample and reference piece, respectively. The average result of final diameters of four specimen samples was taken and used to calculate the corrosion index.

2.2 Static Crucible Test

For the static corrosion cup test, PSR-993 refractory slip was cast into cubed (75mm x 75mm x 75 mm) static corrosion cup test plaster moulds with a 25 (±0.02) mm diameter and 25 (±0.02) mm depth core/cavity in the middle; and left overnight. After 24h, the green casts static cup test samples were dried and sintered at 1500 °C in static air at ambient pressure. Alumina has poor thermal shock properties and hence, the heating and cooling rate was maintained at 50 ºC h^{-1} during the sintering process. A standard SLS glass, sieved through a 600 µm sieve, was placed into the core of cup samples and filled up to the top. The entire block of refractory containing SLS glass inside the cavity was heated to 1370 ºC for 72h. The heating and cooling rate was maintained at 50 ºC h-1. The slow heating rate was maintained to limit formation and expansion of bubbles as well as foaming in the glass melt from air initially trapped between the glass cullet particles. Foaming due the trapped air can result in the melt rising and spilling above the rim upper rim of the crucible. A slower cooling rate was adopted to allow saturation and equilibrium to be reached and new phases that may form at the interface to be evaluated and compared with the hot corrosion behaviour of the dynamic test.

After the duration of the test, the static cup test refractory samples were cooled and axially sectioned to reveal the glass-refractory interface and evaluate the glass-refractory interaction for further examination.

2.3 Sample Characterisation

For SEM analysis, the regions between, below the melt-line and the bottom end of the finger samples were selected for analysis. For the static finger samples, the same refractory-glass region, from the vertical side wall, just below the glass meniscus/melt line to the bottom horizontal upward facing wall; was sectioned and analysed. The cross-sectional surfaces consisting of glass-refractory interface of samples before and after the dynamic corrosion test at 1370 ºC for 72 hrs revolving at 15 rpm were analysed using X-ray diffraction (XRD, P'Analytical X'Pert MPD, Netherlands) employing Cu Kα radiation (1.5418 Å) at ambient temperature. The microstructures of the cross-sectional surface of the samples obtained after dynamic corrosion test and static crucible test were characterised by Scanning Electron Microscopy and Energy Dispersive X-ray Spectroscopy (SEM-EDS, FEG-SEM LEO Gemini 1530).

3 Results and Discussion

3.1 Dynamic corrosion test

Figure 2 shows a typical example of PSR-993 samples that have been withdrawn from molten SLS glass for further inspection and analysis after dynamic corrosion testing. The samples were tested at 1370 ºC for 72 hours at 15 rpm (1884 mm min^{-1}) rotation speed. The PSR-993, high purity α-Al_2O_3, shows excellent corrosion resistance to SLS glass compared with AZS and Cr_2O_3-containing refractories [6, 7]. Some superficial spherical pores were observed on the sample surface because of air bubbles trapped in the slip during casting and drying process. The length of the samples that was submerged in molten glass can be easily identified by the layer of residual condensed glass adhering to the sample surface as seen in Figure 2. Examination of the finger samples in Figure 2 show that there is no significant change in the width or diameters of the region above the glass melt line and that which was submerged within the glass melt. There is no pitting or any noticeable material loss in these regions highlighting excellent corrosion resistance of the alumina refractory to SLS glass compared with AZS and Cr_2O_3-containing refractories [6, 7]. However, clear volume change is observed at the refractory-glass interface and refractory-glass-air triple interface relative to the dimension of the original samples. More pronounced corrosion is observed at the triple phase boundary (TPB) due to the well-known Marangoni effect [13]. The diameter of the samples is measured after the test at the TPB to calculate the corrosion resistance of the sample based on the difference between the diameter of the sample before and after the test at fixed temperature, time and rotation speed using Equation 1.

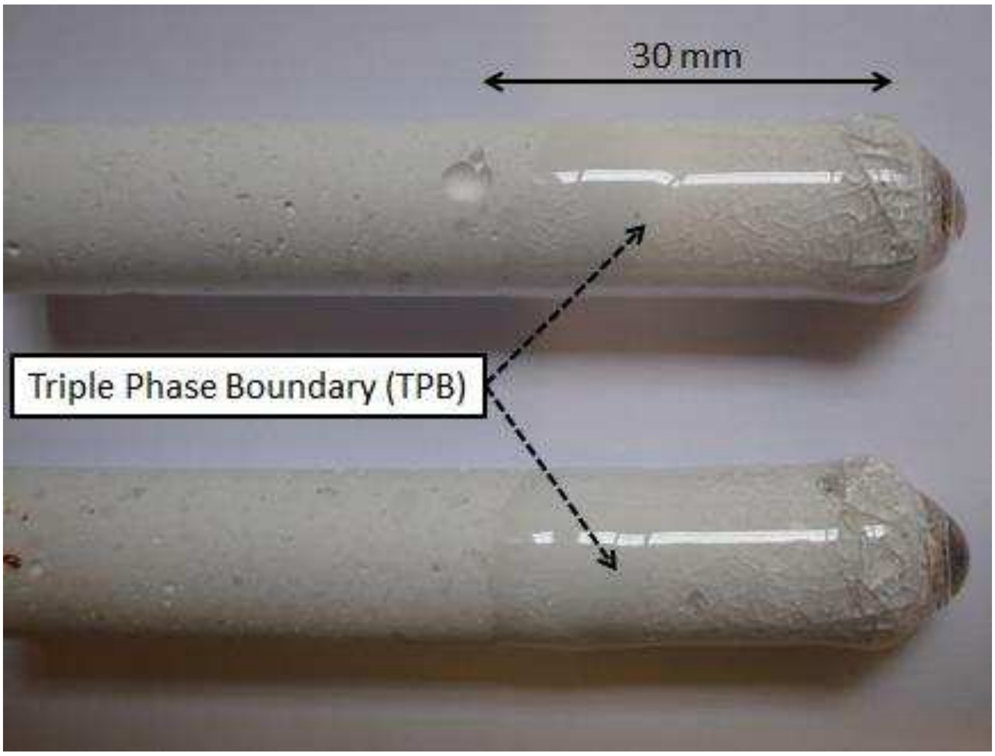

Figure 2: PSR-993 samples after dynamic corrosion test at 1370 ºC for 72 hrs at 15 rpm (1884 mm min^{-1}) rotation speed using SLS cullet.

As shown in Figure 3, the final volume of the sample after dynamic corrosion test for different time lengths, at different rotation speeds and temperatures have been calculated using the measurements of reference sample. This data of reference sample was obtained according to the ASTM standard [12] at 1370 ºC for 72 hrs with no rotation (i.e. in static condition). The average final volume of the sample after the static test (96.9 ± 0.01%) was found to be corresponding to the reduction of sample diameter from 15.28 ± 0.02 to 14.21 ± 0.03 mm. Therefore, the average diameter of PSR-993 samples was reduced by

~1 mm relative to the static corrosion test at 1370 ºC for 72 hrs. Figure 3A shows that, as rotation speed increase, the average volume change increases due to simultaneous erosion and corrosion of the sample in contact with the molten SLS glass. It is believed and has been shown that the enhanced corrosion of refractories, as seen in Figure 3A, is due to the chemical reaction between Na+ / Ca2+ cations in SLS glass and α-Al2O3 in PSR-993 at high temperature [2, 8]. The erosion is caused by the flow of viscous molten glass continuously washing the surface of the refractory because of the rotation of samples in glass. These two processes act synergistically on the sample. Hence, the relative final volume of PSR-993 samples reaches a minimum (~96.2%) compared with the reference sample when the rotation speed is set at 15 rpm. This is equivalent to a linear flow rate of approximately 1884 mm min^{-1} which is approximately 10 times greater than that employed in the glass industry, usually 180 mm min^{-1}.

Moreover, a linear relationship is observed between the relative volume remaining and the reaction time lengths of PSR-993 samples remaining after the dynamic corrosion test as seen in Figure 3B. The specimen tested at 1370 ºC for 24 hours at 628 mm min^{-1} (5 rpm) rotation speed shows more corrosion resistance compared to the reference sample. The relative remaining volume is calculated as ~99.6 %. This is because of the short length of reaction time period taken of 24 hrs; which is considerably shorter than the standard reaction test period of 72 hrs, as shown in Figure 3B. The relative final volume decreases linearly as the reaction time length increases. It reaches to a minimum value of ~97.3% when the reaction time equals 72 hrs, same as the reaction time length of the reference test. The difference between the test sample and the reference sample at a fixed temperature of 1370 ºC and time of 72 hours is due to erosion as a result of continuously rotating the samples in molten glass at 5 rpm during the experiment.

A polynomial relationship is observed between the relative final volume and the temperature of PSR-993 samples after the dynamic corrosion test (see Figure 3B). The relative final volume of specimen tested at 1420 ºC for 72 hrs at 15 rpm (1880 mm min^{-1}) rotation speed is calculated as ~95.1%. The relative final volume decreases as the temperature increases and reaches a minimum value of ~92.6% at 1470 ºC. These measurements obtained from Figure 3B are also used to calculate the dynamic corrosion rate which is plotted in Figure 3C.

Figure 3C shows an exponential relationship between the dynamic corrosion rate and temperature. The dynamic corrosion rate can be expressed by the following equation:

$$Dynamic\ corrosion\ rate = \frac{\pi\left[\frac{(D_i - D_f)}{2}\right]^2 \Delta l}{t} \qquad (2)$$

Where, D_i and D_f are the initial and final diameter of the test sample, respectively. The change in length of the specimen Δl = 1 mm and reaction time t = 72 hrs, respectively. As shown in Figure 3C, the dynamic corrosion rate at different temperatures (1370, 1420, 1460 and 1470 ºC) is approximately equal to 0.0029, 0.0048, 0.0075 and 0.0084 mm^{3}hr^{-1}, respectively. The corrosion rate of PSR-993 (α-Al_2O_3) refractory approximately doubles for every 50 ºC increase in temperature. These findings agree reasonably well with the reports in the literature [14]. An Arrhenius relationship has been obtained between the natural logarithm of the dynamic corrosion rate and 103/T (K) as shown in Figure 3D given by the equation;

Ln (corrosion rate) = -29780/T (K) + 12.29. ……………………………………(3)

The activation energy for the corrosion of α-Al2O3 bonded refractories in molten SLS glass is calculated as 247.6 kJ mol^{-1}. However, it should be noted that the standard glass flow rate in glass industry is approximately 180 mm min^{-1}. Hence, the true dynamic corrosion rate of PSR-993 refractory in contact with SLS glass is about 0.0003 $mm^3 hr^{-1}$ at 1370 ºC with standard industrial glass flow rate. Based on this calculation, the thickness of the refractory reduces approximately 30 mm at the triple phase boundary (TPB) for a typical glass production channel made from PSR-993 refractory at 1370 ºC in full service over a period of 10 years.

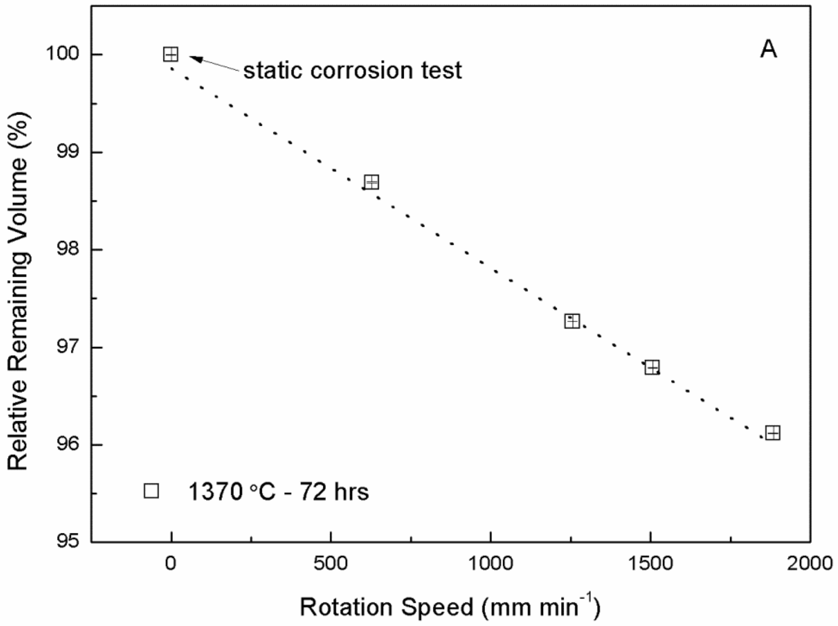

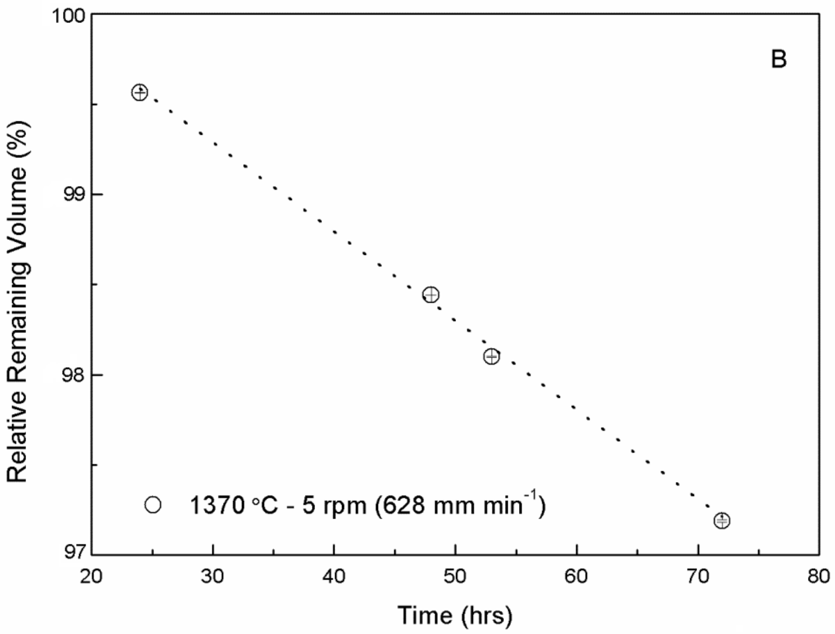
B
Relative Remaining Volume (%)
100
99
98
97
20
30
40
50
60
70
80
Time (hrs)
○ 1370 °C - 5 rpm (628 mm min^{-1})

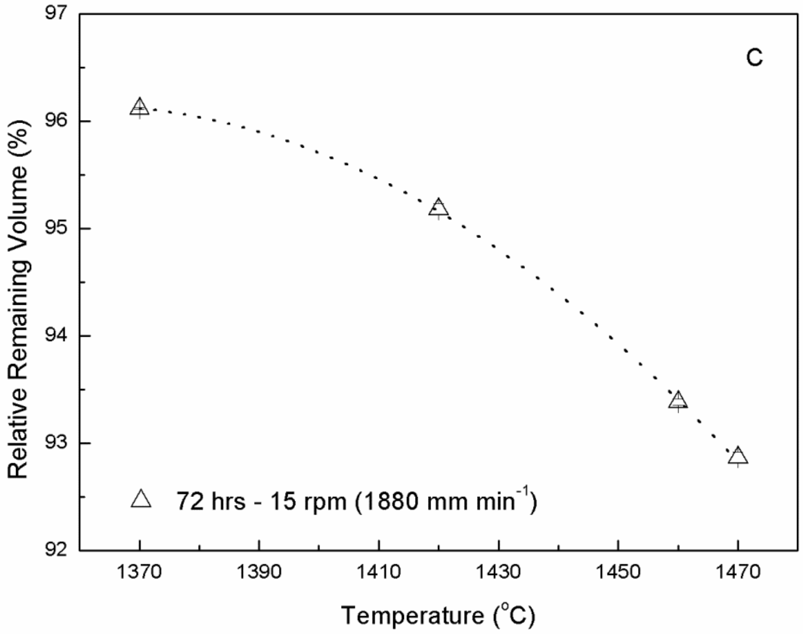
C
Relative Remaining Volume (%)
97
96
95
94
93
92
1370
1390
1410
1430
1450
1470
Temperature (°C)
△ 72 hrs - 15 rpm (1880 mm min^{-1})

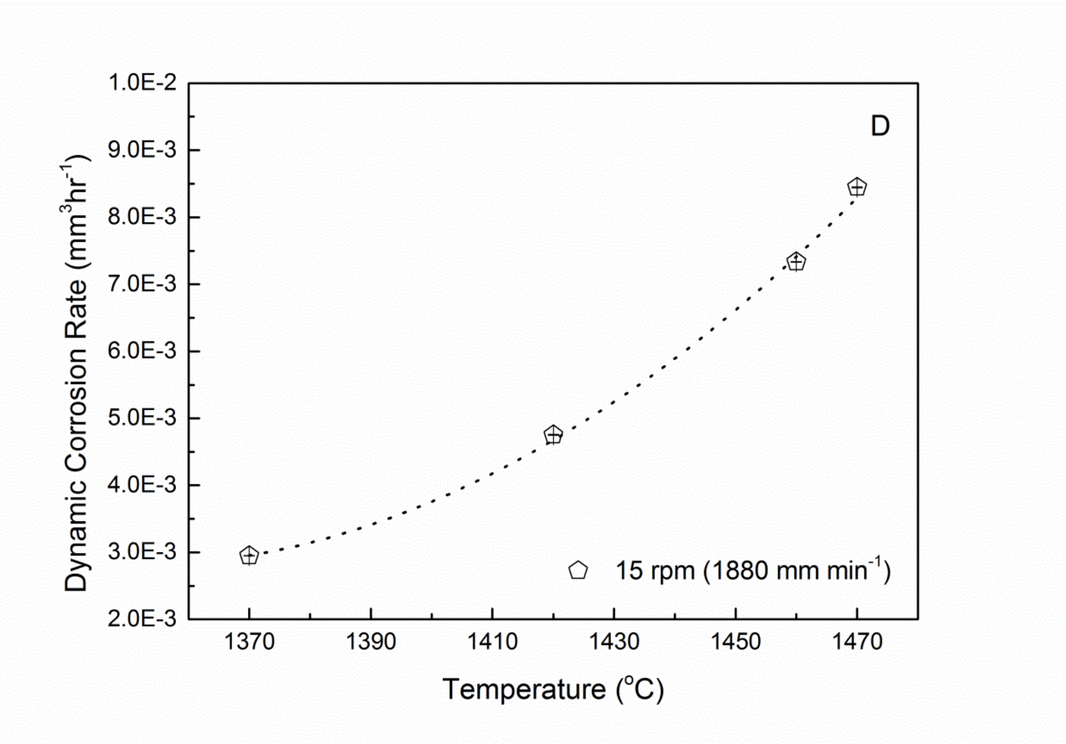

Figure 3: Relative final volume and dynamic corrosion rate of PSR-993 after dynamic corrosion test at different conditions. **A** is various rotation speeds at 1370 ºC for 72 hrs, **B** is various reaction time lengths at 1370 ºC with 5 rpm rotation speed, **C** is various temperatures with 15 rpm for 72 hrs and **D** is dynamic corrosion rate at various temperatures with 15 rpm for 72 hrs, respectively.

3.2 Static crucible test

Figure 4 shows one of the axially sectioned static cup test samples highlighting the glass-refractory interface and compatibility. Small amount of molten glass is seen to adhere on the side of the cup as a thin layer after cooling. This is a typically observed in the static crucible test and occurs because of the creep of molten glass and the shrinkage in volume of glass when cooled from liquid to solid phase. Some spherical pits are also observed on the cross-sectional surface of the refractory sample due to the air bubbles trapped during slip casting, drying and sintering process. Slight corrosion is observed at the refractory-glass-air triple interface (TPB).

Figure 4 further reveals a pale-yellow reaction zone at the refractory-glass interface on analysis after the test. Glass constituents have diffused into the refractory region altering the microstructure to form a penetration/reaction zone. The width of the penetration/reaction zone is shown in figure 4 as 551, 9 µm. This is because of the net result of both physical penetration of glass into the refractory sample and chemical reaction between the constituents of glass and refractory material. The chemical reactions are mainly between the alkali and alkaline earth metal cations, such as Na+ and Ca2+ present in SLS glass and amphoteric alumina in the refractory material to form new compounds at the refractory-glass interface during the prolonged (72 hr) high-temperature (1370 ºC) experiment. Moreover, molten glass easily penetrates the pores of the sintered refractory sample, having up to 16% porosity in the commercial samples, through the interconnected porosity. The PSR-993 refractory interface profile is smooth and straight highlighting the excellent glass corrosion resistance of the PS-993 refractory to the SLS glass

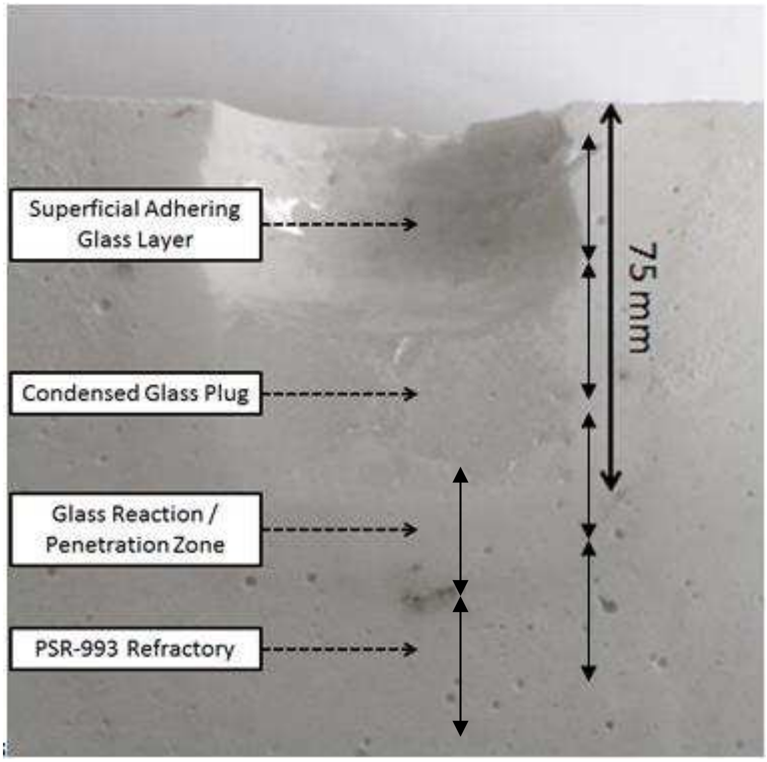

Figure 4: Static corrosion crucible test of PSR-993 samples at 1370 ºC for 72 hrs using SLS cullets. Approximate lengths of each zone are shown in the diagram.

3.3 Characterization

Figure 5 shows the XRD pattern of the PSR-993 sample before and after dynamic corrosion test at 1370 ºC for 72 hours and 15 rpm rotation speed. The XRD patterns could be entirely indexed with the reference pattern (α-Al_2O_3 04-005-4213) available in the literature marked at the top of figure. However, it can be seen in Figure 5 that the intensity of the α-Al_2O_3 peaks has uniformly reduced in the sample after corrosion test compared with that before the corrosion test. This can be attributed to the fact that as corrosion of the refractory proceeds, the matric region is readily attacked by the Na^+, Ca^{2+} and SiO_4^- from the glass. Soda has more penetrating effect than the other glass constituents. The soda reacts with the high alumina to form beta alumina which is dissolved as more of small alpha-alumina matrix grains are dissolved and depleted to form a sodium aluminosilicate glass at the interface and surrounding the grog alumina grains in the reaction or penetration zone. With increased rotation speed and thereby forced glass convection, the glassy boundary layer is washed off the interface and the refractory is exposed to fresh glass and more glass attack.

More importantly, no detectable traces of impurities or additional new phases are observed after the dynamic corrosion test even though the reaction or diffusion zone is clearly visible in Figure 4. This may be due to the formation of traces of Na^+ and Ca^{2+} ion containing alumina compounds present in the sample that is below the detection limit of XRD. A slightly mis-match between the actual peaks from both samples and the reference is observed as shown in Figure 5 due to the sample displacement during XRD scanning.

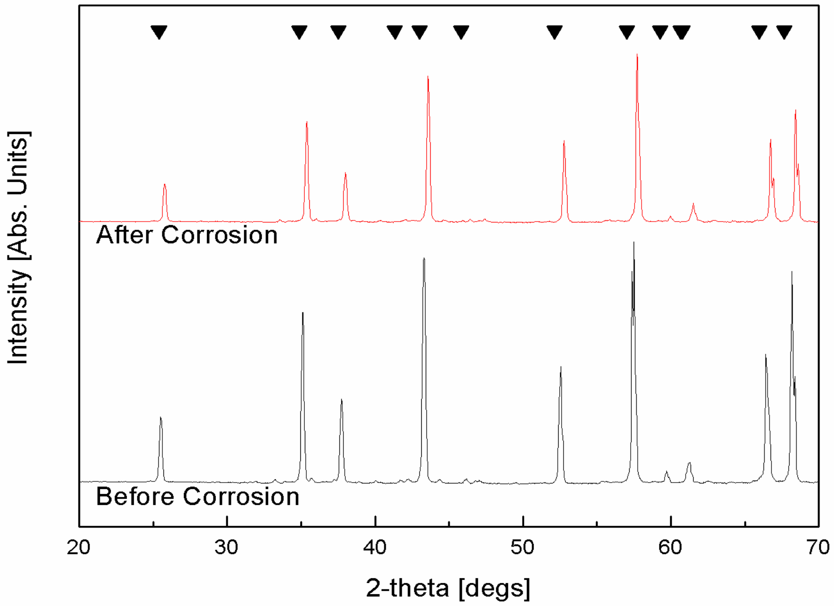

Figure 5: XRD of PSR-993 before and after dynamic corrosion test at 1370 °C for 72 hrs with 15 rpm rotation speed. Tick marks for reference pattern of α-Al_2O_3, ICDD 04-005-4213, are shown at the top of the figure.

No nepheline is formed in high alumina refractories and none was detectable in our study. This is in agreement with results by Farris and Allen [15] where in 70% and 90% high fired alumina refractories no nepheline products were detectable. Also, composition variation studies by Vienna et al [16] and Hong et al [17], showed that glasses with $SiO_2/(SiO_2+Na_2O+ Al_2O_3)$ mass fraction > 0.62 do not precipitate nepheline as their primary phase. This is in good agreement with our experimental results where the high alumina refractory solved at the interface did not precipitate nepheline.

SEM analysis of the cross-sectional surface of PSR-993 samples obtained after dynamic corrosion test at 1370 °C for 72 hrs with 15 rpm rotation speed is shown in Figure 6. As seen in the figure, a clear and sharp interface is observed between the glass and refractory. Some scratch lines are seen in the glass layer due to chipping of glass during the sample preparation. However, no reaction zone is observed in this sample. This is due to the fact that the Na^+ and Ca^{2+} containing alumina compounds are either washed away by continuous rotation of test sample in molten glass or they are present below the detection limit of SEM analysis.

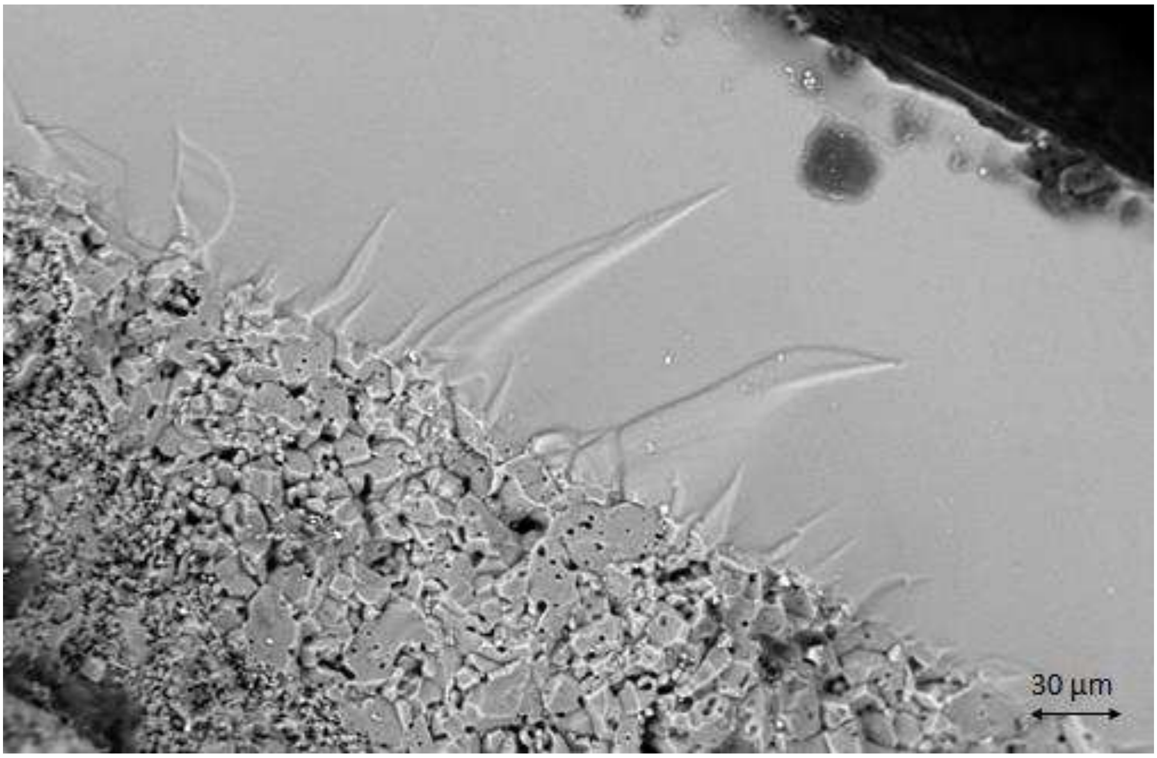

Figure 6. SEM of the refractory-glass interface of PSR-993 after dynamic corrosion test at 1370 ºC for 72 hrs with 15 rpm rotation speed.

Figure 7 shows the EDS analysis of the cross-sectional surface of the PSR-993 samples using elemental mapping. The silicon rich glass (Si^{4+}) and aluminium rich refractory (Al^{3+}) layer can be clearly identified in the figure. An extremely small trace of Al^{3+} is also observed in the glass layer and Ca^{2+}, Na^+ and Si^{4+} in alumina region indicating that aluminium may be diffusing into the glass layer and silicon, calcium and sodium in to the refractory layer as a result of combined corrosion and erosion process taking place during the test campaign. Based on the thermodynamic consideration, Na and Ca diffusion could occur due to the reaction between the α-Al_2O_3 in the refractory and Na^+ / Ca^{2+} ions present in molten glass by the virtue of the following two reactions.

$$Na_2O + 9.5Al_2O_3 \xrightarrow{1643K} Na_2O \cdot 9.5Al_2O_3 \tag{3}$$

$$\Delta G^0_{1643K} = -224.2 \pm 0.60\ kJ\ mol^{-1} \tag{4}$$

and,

$$CaO + 6Al_2O_3 \xrightarrow{1643K} CaO \cdot 6Al_2O_3 \tag{5}$$

$$\Delta G^0_{1643K} = -78.5\ \pm 1.35\ kJ\ mol^{-1} \tag{6}$$

The Gibbs energy change for reaction (3) and (5) at 1370 ºC (1643 K) is -224.2 ± 0.60 kJ mol^{-1} [18,19] and -78.55 ± 1.35 kJ mol^{-1} [20], respectively indicating that these two phases are thermodynamically stable at elevated temperature and oxygen potentials prevailing in molten SLS glass. This data has been reviewed recently by Spear and Allendorf [8] and is in reasonably good agreement with the previous experimental determinations [18-20]. Erosion of refractory may occur due to the formation of thermodynamically stable Na^+ / Ca^{2+} containing alumina rich compounds as discussed earlier which in turn could lead to the formation of loosely bonded α-Al_2O_3 matrix within PSR-993 refractory. The loosely bonded ceramic phase in PSR-993 could be easily washed away by continuous rotation of samples in viscous glass melt at 1370 °C leading to erosion of refractory. On the other hand, no Si^{4+} containing phases could be detected (see Figure 7) in the refractory layer indicating that PSR993 (α-Al_2O_3) is thermodynamically stable in contact with silica at 1370 ºC. However, a small amount of Na^+ and Ca^{2+} is observed (see Figure 7) in the refractory layer as seen in the elemental maps of the interface layer between SLS glass and PSR-993. This is due to possible chemical corrosion reaction between alumina and SLS glass containing Na^+ and Ca^{2+} at high temperature as mentioned earlier. Oxygen is observed in both layers by EDS analysis (see Figure 7) since it is present in the constituent oxides of both SLS glass and in PSR-993 refractory sample.

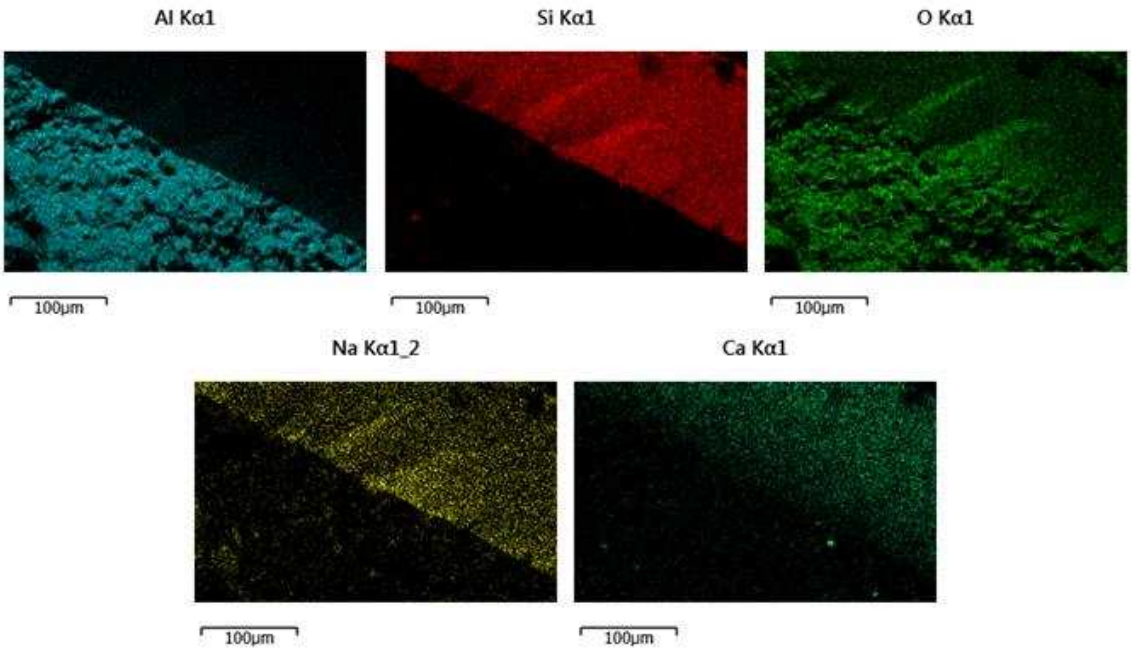

Figure 7. Elemental maps of the refractory-glass interface of PSR-993 after dynamic corrosion test at 1370 ºC for 72 hrs with 15 rpm rotation speed.

Figure 8 shows the SEM analysis of the glass-refractory interface of PSR-993 samples after static crucible test at 1370 ºC for 72 hours. The reaction zone of the sample after test has been found to be 551.9 μm wide using high magnification SEM (see Figure 8A). This result agrees reasonably well with that obtained using dynamic corrosion test at 0 rpm rotation speed (~1 mm in diameter), as described in the section earlier related to Figure 3A.

In figure 8, a clean, smooth interface is also observed between the glass and refractory showing that PSR-993 has high corrosion resistance against SLS glass. The microcracks observed in the reaction zone may because of the difference in thermal expansion coefficient between Na^+ / Ca^{2+} contain alumina compounds present in the reaction zone and α-Al_2O_3 of the sample. Furthermore, it is also possible that some microcracks could have been introduced in the sample during cutting a small sample out of the bulk ceramic test crucible and sample preparation for SEM-EDS examination. Low magnification SEM of the sample is shown in Figure 8B.

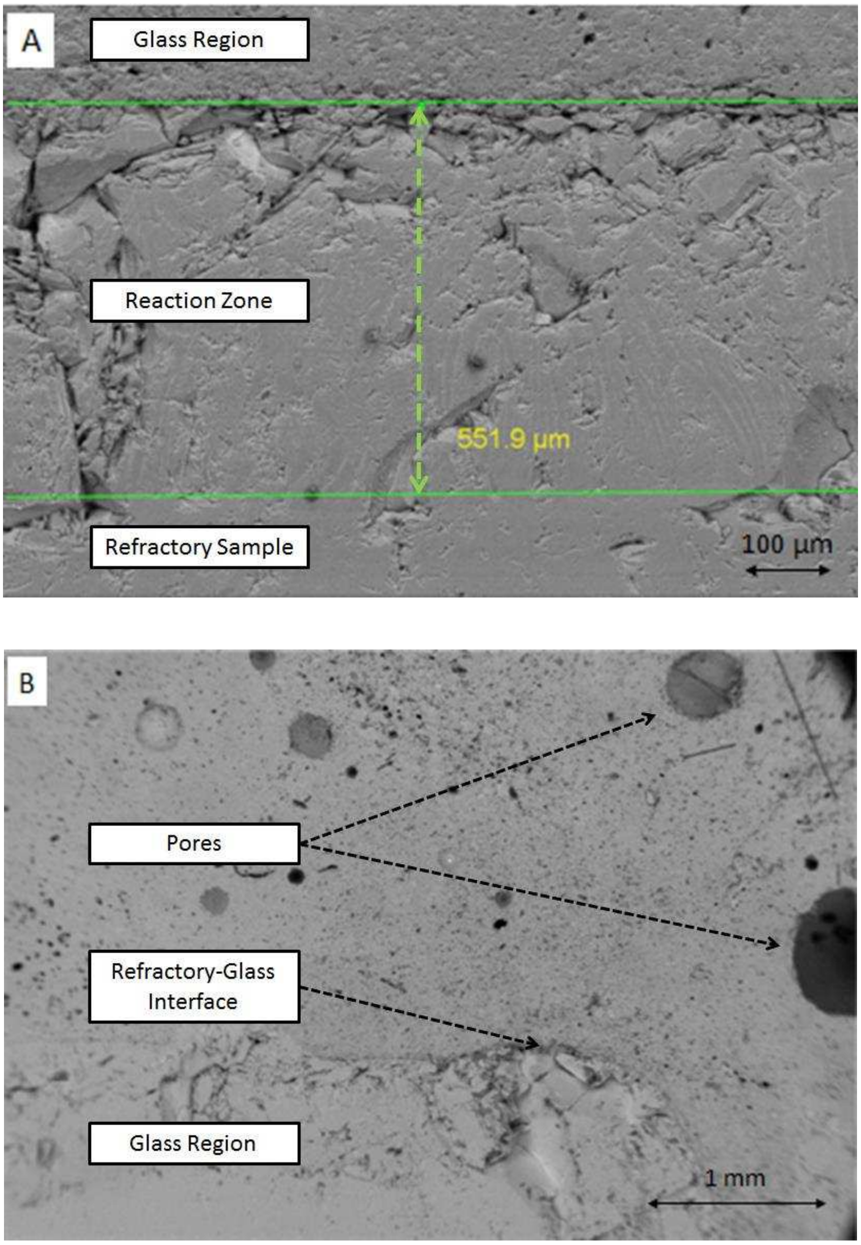

Figure 8. SEM image of the refractory-glass interface of PSR-993 after static corrosion test (crucible test) at 1370 °C for 72 hrs. **A** is high magnification and **B** is low magnification image, respectively. Note that spherical objects in refractory zone are pores of varying diameters.

Figure 9 shows the glass-refractory interface of PSR-993 after static crucible test at 1370 ºC for 72 hours is analyzed by EDS. Strong Al^{3+} signal is observed in the refractory layer showing that PSR-993 has a good corrosion resistance. However, small amount of Al^{3+} is detected in the glass layer. Moreover, traces of Si^{4+} ion is observed in the refractory layer (see Figure 9) indicating possible penetration or migration of glass constituents into the refractory zone through molten glass penetrating into the micropores within the refractory sample after 72 hours of glass contact in static condition. Finally, a decreasing gradient of both Na^+ and Ca^{2+} ions from the glass to the refractory layer is observed, as seen in Figure 9, indicating that the corrosion is indeed occurring at the glass-refractory interface which leads to the formation of reaction zone shown in Figure 8A and the presence of small amount of Al^{3+} detected in the glass layer from the dissolved α-Al_2O_3.

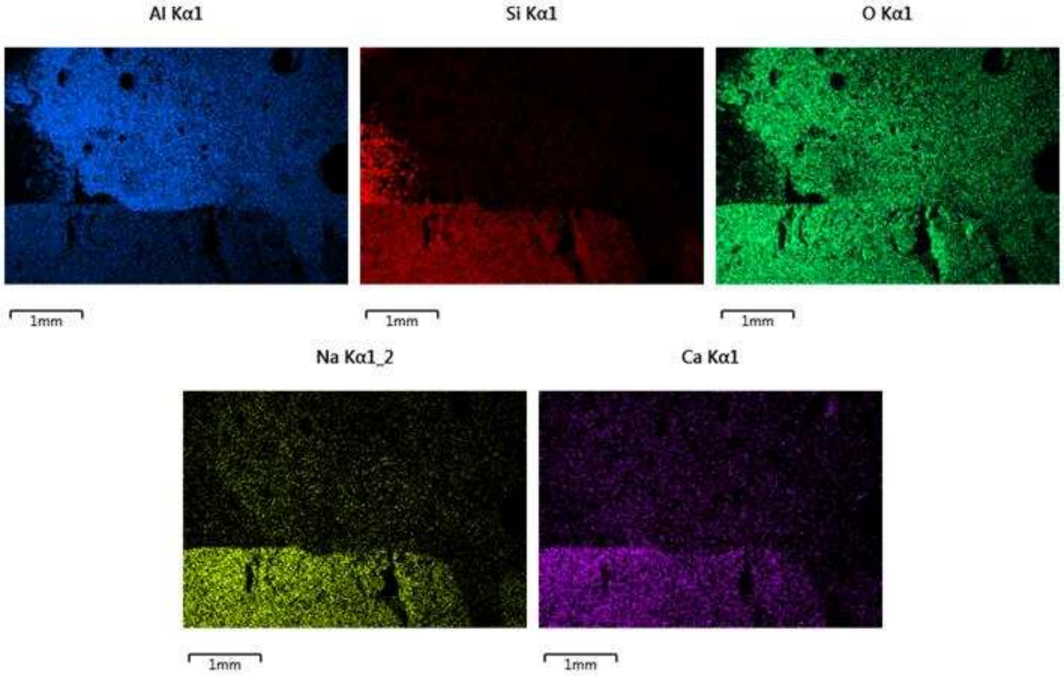

Figure 9. Elemental maps of the cross-sectional surface of PSR-993 after static corrosion test (crucible test) at 1370 °C for 72 hrs.

4 Conclusion

In this investigation, the corrosion behaviour of high purity α-Al_2O_3 (PSR-993) has been studied using dynamic corrosion test at various rotation speed, reaction time lengths and temperatures. The results show excellent agreement with those obtained by static crucible test at 1370 ºC for 72 hours using commercial standard SLS glass. The microstructures of the cross-sectional surfaces of the samples obtained from both dynamic corrosion test and static crucible test indicate that small amount of Na^+ and Ca^{2+} containing alumina compounds are formed at the refractory-glass interface. This has been confirmed by the high thermodynamic stability of compounds such as Na-β-Al_2O_3 and CaO·6Al_2O_3 reported in the literature. However, the rate of formation of these compounds appear to be very sluggish due to the low chemical potential gradient of Na_2O and CaO between the SLS glass and Na-β-Al_2O_3 and CaO·6Al_2O_3 at 1370 °C, respectively. In conclusion, the present investigation confirms that a high corrosion resistant reaction bonded α-Al_2O_3 rich PSR-993 is an ideal glass contact refractory material for glass processing and manufacturing industry.

5 Acknowledgments

I would like to thank Parkinson Spencer Refractories Ltd, Halifax (PSR) for supplying their commercial raw materials for this study.

Declarations of interest: None.

6 References

[1] D.E. Parkinson, "Feeder and forehearth refractories," Glass Tech., **29** [5] 173-6 (1988).

[2] G.S. Rossikhina, V.V. Podkholyuzin, E.A. Doroganov and V.V. Doroganov, "Corrosion resistance of refractories made from low-cement concretes for glass making," Glass and Ceram., **63** [11-12] 24-8 (2006)

[3] G. Ye, T. Troczynski, "Hydration of hydratable alumina in the presence of various forms of MgO," Ceram. Int., **32** [3] 257-62 (2006).

[4] F.A. Cardoso, M.D.M. Innocentini, M.M. Akiyoshi, V.C. Pandolfelli, “Effect of curing time on the properties of CAC bonded refractory castables,” J. Euro. Ceram. Soc., **24** [7] 2073–8 (2004).

[5] C. Gogtasa, H.F. Lopeza, K. Sobolev, “Role of cement content on the properties of self-flowing Al_2O_3 refractory castables,” J. Euro. Ceram. Soc., **34** [5] 1365-73 (2014).

[6] C. Baudín, E. Criado, J.J. Bakali, P. Pena, “Dynamic corrosion of Al_2O_3–ZrO_2–SiO_2 and Cr_2O_3-containing refractories by molten frits. Part I: Macroscopic analysis,” J. Euro. Ceram. Soc., **31** [5] 697-703 (2011).

[7] P. Pena, E. Criado, J.J. Bakali, C. Baudín, “Dynamic corrosion of Al_2O_3–ZrO_2–SiO_2 and Cr_2O_3-containing refractories by molten frits. Part II: Microstructural study,” J. Euro. Ceram. Soc., **31** [5] 705-14 (2011).

[8] K.E. Spear, M.D. Allendorf, “Thermodynamic analysis of alumina refractory corrosion by sodium or potassium hydroxide in glass melting furnaces,” J. Electrochem. Soc., **149** [12] 551-9 (2002).

[9] C. Aksel, “The microstructural features of an alumina–mullite–zirconia refractory material corroded by molten glass,” Ceram. Int., **29** [3] 305-9 (2002).

[10] T. Hirata, T. Morimoto, A. Deguchi, N. Uchida, “Corrosion Resistance of Alumina-Chromia Ceramic Materials Against Molten Slag,” Mater. Trans., **43** [10] 2561-7 (2002).

[11] C.G. Aneziris, E.M. Pfaff, H.R. Maier, “Corrosion mechanisms of low porosity ZrO_2 based materials during near net shape steel casting,” J. Euro. Ceram. Soc., **20** [2] 159-68 (2000).

[12] ASTM C621-84, “Standard Test Method for Isothermal Corrosion Resistance of Refractories to Molten Glass,” Ann. Book of ASTM Stand., (2009)

[13] McCauley RAM, Corrosion of Ceramics and Composite Materials, Marcel Dekker Inc., New York, 2004.

[14] S. Jansson, V. Brabie, P. Jönsson, “Corrosion mechanism and kinetic behaviour of MgO-C refractory materials in contact with CaO-Al_2O_3-SiO_2-MgO slag,” Scand. J. Metall., **34** [5] 283-92 (2005).

[15] R. Farris and J. Allen, Aluminous refractories – alkali reactions, Iron and Steel Engineering 50 (2) (1973) 67-74.

[16] John D. Vienna, Compositional Models of Glass/Melt Properties and their Use for Glass Formulation, Procedia Materials Science,Volume 7,(2014),pp 148-155,

[17] Li, Hong & R. Hrma, Pavel & Vienna, John & Qian, Maoxu & Su, Yali & E Smith, Donald. “Effects of $A1_2O_3$, B_2O_3, Na_2O, and SiO_2 on Nepheline Formation in

Borosilicate Glasses: Chemical and Physical Correlations". Journal of Non-Crystalline Solids. 331. (2003). pp 202-216.

[18] K. T. Jacob, K. Swaminathan, O. M. Sreedharan, "Potentiometric determination of activities in the two-phase fields of the system Na_2O-α-Al_2O_3," Electrochem. Acta, **36** [5/6] 791-8 (1991).

[19] G. M. Kale, "Na_2O-Al_2O_3 system: Activity of Na_2O in (α+β)- and (β+β″)-Al_2O_3," Metall. Trans. B, **23B** [12] 833-9 (1992).

[20] M. Allibert, C. Chatillon, K. T. Jacob, R. Lourtau, "Mass-spectrometric and electrochemical studies of thermodynamic properties of liquid and solid phases in the system CaO-Al_2O_3," J. Electrochem. Soc., **64** [5], 307-14 (1981).

7 List of Figures

Figure 1. Part of the dynamic corrosion test rig. **A** is PSR-993 samples about to be immersed in molten SLS glass at 1370 °C during dynamic corrosion test and **B** is the ceramic sample holder with PSR-993 fingers being withdrawn from molten glass after dynamic corrosion test, respectively.

Figure 2. PSR-993 samples after dynamic corrosion test at 1370 °C for 72 hrs at 15 rpm (1884 mm min^{-1}) rotation speed using SLS cullet.

Figure 3. Relative final volume and dynamic corrosion rate of PSR-993 after dynamic corrosion test at different conditions. **A** is various rotation speeds at 1370 °C for 72 hrs, **B** is various reaction time lengths at 1370 °C with 5 rpm rotation speed, **C** is various temperatures with 15 rpm for 72 hrs and **D** is dynamic corrosion rate at various temperatures with 15 rpm for 72 hrs, respectively.

Figure 4. Static corrosion crucible test of PSR-993 samples at 1370 °C for 72 hrs using SLS cullet.

Figure 5. XRD of PSR-993 before and after dynamic corrosion test at 1370 ºC for 72 hrs with 15 rpm rotation speed. Tick marks for reference pattern of α-Al_2O_3, ICDD 04-005-4213, are shown at the top of the figure.

Figure 6. SEM of the refractory-glass interface of PSR-993 after dynamic corrosion test at 1370 ºC for 72 hrs with 15 rpm rotation speed.

Figure 7. Elemental maps of the refractory-glass interface of PSR-993 after dynamic corrosion test at 1370 ºC for 72 hrs with 15 rpm rotation speed.

Figure 8. SEM image of the refractory-glass interface of PSR-993 after static corrosion test (crucible test) at 1370 ºC for 72 hrs. **A** is high magnification and **B** is low magnification image, respectively. Note that spherical objects in refractory zone are pores of varying diameters.

Figure 9. Elemental maps of the cross-sectional surface of PSR-993 after static corrosion test (crucible test) at 1370 ºC for 72 hrs.

8 List of Table

Table 1. Chemical constituents of the soda-lime silica glass and PSR-993 test specimen.

Oxides (wt%)	**SiO_2**	**Na_2O**	**CaO**	**Al_2O_3**	**MgO**	**K_2O**	**Others**
SLS	71.53	12.78	10.78	1.53	1.41	0.59	1.38
PSR-993	-	-	-	99.70	-	-	0.30